

AVERAGE PROPERTIES OF THE TIME BEHAVIOUR OF GAMMA-RAY BURSTS

Boris Stern^{1,2}, Roland Svensson² and Juri Poutanen^{2,3}¹Institute for Nuclear Research, Moscow²Stockholm Observatory, Saltsjöbaden, Sweden³Uppsala Observatory, Uppsala, Sweden

ABSTRACT

Time profiles of gamma ray bursts (GRBs) are extremely diverse in their durations, morphologies, and complexity. Nevertheless, the average peak-aligned profile of all bursts detected by BATSE with sufficient data quality has a simple “stretched” exponential shape, $F \propto \exp[-(t/t_0)^{1/3}]$, where t is the time measured from the time for the peak flux, F_p , of the event, and t_0 is a time constant. We study the behaviour of t_0 of both the post-peak and the pre-peak slopes of the average time profile as a function of the peak brightness range of the burst sample. We found that the post-peak slope shows time dilation when comparing bright and dim bursts, while the pre-peak slope hardly changes. Thus dimmer bursts have a different shape – they are more asymmetric. This shape-brightness correlation is observed at a 99.6% confidence level. Such a correlation has a natural explanation within the pulse avalanche model, which is briefly described. Complex events, consisting of many pulses are more symmetric and are intrinsically brighter. Bursts consisting of one or a few pulses are intrinsically weaker and more asymmetric. For such a correlation to be observable requires that the luminosity distance distribution of GRBs to be different from a power-law.

Keywords: Gamma-ray bursts, Methods: Data analysis.

1. INTRODUCTION

Stern (1996) found that the average peak-aligned time profile of GRBs (the procedure of peak-alignment was pioneered by Mitrofanov et al. 1994, 1995) in the BATSE-2 catalog has a simple “stretched” exponential shape, $\langle F/F_p \rangle = \exp[-(t/t_0)^{1/3}]$, where t is the time since the peak flux, F_p , of the event, and t_0 is a constant ranging from 0.3 s for strong bursts to ~ 1 s for dim bursts. This dependence of t_0 on brightness can be interpreted as a cosmological time dilation (e.g., Paczyński 1992; Piran 1992).

Such a simple average time profile is remarkable con-

sidering the diverse and chaotic behavior of the individual time profiles of GRBs. On the other hand, the simple shape of the average time profile gives an excellent opportunity to study effects such as time dilation.

Here, we study the two slopes of the average time profile for a larger sample of GRBs and with a more accurate treatment of the background than was done in Stern (1996). Another advantage we now have is the access to the pulse avalanche model developed by Stern & Svensson (1996) which successfully describes many statistical properties of GRBs including the stretched exponential shape of the profile and, of particular importance for the present work, the rms variance of individual time profiles. This means that we can rely on this model when estimating the errors of stretched exponential fits, which in turn gives us reliable estimates of the significance levels of the observed effects.

2. DATA PROCESSING

This work is based on data obtained from the publicly available BATSE database at Goddard Space Flight Center. Our sample includes bursts up to trigger number 3745. We used the 0.064 s and 1.024 s time resolution data from the Large Area Detectors (LAD). All time profiles were constructed with 64 ms time resolution together with pre and post-burst extensions of 1024 ms time resolution. All background fits were done with the 1024 ms data as they cover a wider time interval including the pre-trigger history. The time profiles were studied using count rates in all 4 LAD’s energy channels.

The procedure of background fitting included:

- A visual examination of all bursts including both 64ms and 1 s resolution data.
- All doubtful peaks and count rate variations with χ^2 exceeding that of Poisson noise were analyzed in order to see whether they came from the same direction as the main peak of the burst. This was accomplished by comparing the direction of the eight-component vector consisting of the χ^2 from the eight

LADs for the feature with the direction of the corresponding vector for the main peak.

– Discarding all events with highly variable background as well as those where we were unable to confidently extract sufficiently long intervals of pre-peak and post-peak histories.

– Possible use of widely separated fitting windows to avoid losses of weak GRB signals.

When sorting bursts into brightness groups we used peak fluxes for 64 ms time resolution from the BATSE-3 catalog.

The errors were calculated using the pulse avalanche model. What we need are the statistical errors of the stretched exponential fits to the data. To extract this error directly from the data is very difficult because of strong correlations along the time profile. Instead, we simulated many samples of N events, determined the average time profile for each sample, and then made a stretched exponential fit to each simulated average profile: $F(t) = \beta \exp[-(t/t_0)^{1/3}]$, where t_0 and β are fitting parameters. The same procedure was used as for real data. Finally, the rms errors of the fitting parameters was calculated.

We have two slopes of the profile - the pre-peak (rising) slope and post-peak (decaying) slope. We fitted them simultaneously with different t_0 , denoted here as t_r and t_d , and with a common β . Fitting the simulated samples gave the following relative standard deviations:

$$\sigma(t_{r,d})/t_{r,d} = 0.20\sqrt{100/N}$$

$$\sigma(t_r + t_d)/(t_r + t_d) = 0.19\sqrt{100/N}$$

$$\sigma(t_d/t_r)/(t_d/t_r) = 0.13\sqrt{100/N}$$

Note, that the relative accuracy for the sum of the two time constants is close to that for one time constant, while the accuracy of the asymmetry ratio, t_d/t_r , is markedly better. This is a consequence of a strong correlation between the two slopes – a circumstance that favors the measurement of shape vs. brightness correlations and that complicates the measurement of the time dilation effect. The errors are robust against variations of the parameters of the pulse avalanche model as long as the model gives approximately the correct stretched exponential average profile. The procedure for the data analysis will be described in greater detail in Stern et al. (1997).

3. THE AVERAGE TIME PROFILE FOR DIFFERENT BRIGHTNESS GROUPS

The average peak-aligned profiles for three brightness groups are shown in Figure 1. Both the rising and the decaying profiles are well shaped stretched exponentials for the bright and the medium group, while both profiles are quite deformed for the weakest group. The rising (pre-peak) slope is steeper for all brightness groups, but the asymmetry is increasing when going from the brightest to the dimmest group. The results of our stretched exponential fits are summarized in Table 1 and in Figure 2.

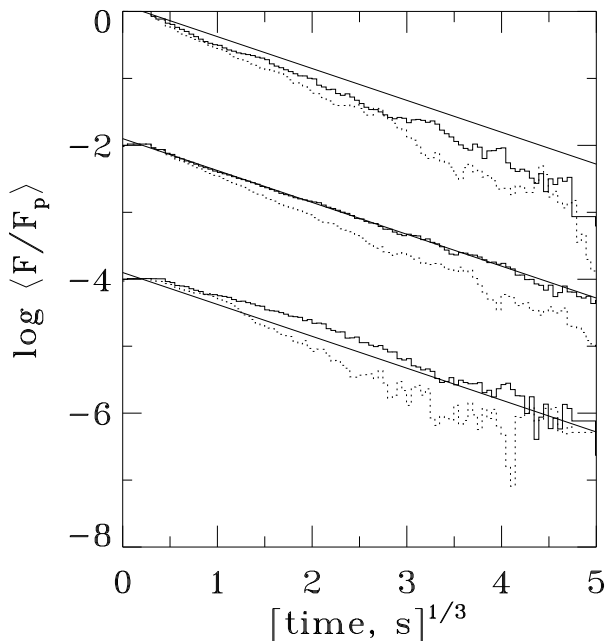


Figure 1: Average peak-aligned time profiles for three brightness groups: 1.) $F_p > 5 \text{ ph cm}^{-2} \text{ s}^{-1}$, 157 GRBs (upper curves); 2.) $0.7 < F_p < 5$, 630 GRBs (middle curves); and 3.) $F_p < 0.7$, 116 GRBs (lower curves). Middle and lower curves are shifted downwards for clarity. Solid and dotted curves represent the average post-peak and pre-peak time profiles, respectively. Straight lines show the best linear fit to the post-peak history of the medium brightness group.

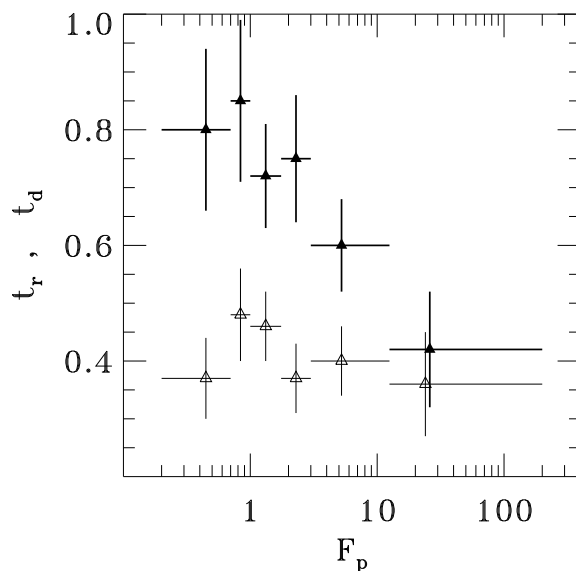


Figure 2: Time constants, t_r and t_d , vs. peak photon flux, F_p , in 64 ms time resolution. Lower and upper crosses represent t_r and t_d for the pre-peak (rising) and post-peak (decaying) average time profile, respectively. Error bars of the time constants correspond to 1σ . Error bars in photon flux represent the width of the brightness groups.

#	Peak flux	N	t_d	t_r	$t_r + t_d$	t_d/t_r
1	12.5 – 200	64	0.42 ± 0.10	0.36 ± 0.09	0.78 ± 0.18	1.17 ± 0.19
2	3 – 12.5	193	0.60 ± 0.08	0.40 ± 0.06	1.00 ± 0.13	1.50 ± 0.11
3	1.75 – 3	159	0.75 ± 0.11	0.37 ± 0.06	1.12 ± 0.16	2.02 ± 0.21
4	1 – 1.75	241	0.72 ± 0.09	0.46 ± 0.06	1.18 ± 0.14	1.56 ± 0.13
5	.7 – 1	139	0.85 ± 0.14	0.48 ± 0.08	1.33 ± 0.21	1.89 ± 0.18
6	0 – .7	116	0.80 ± 0.14	0.37 ± 0.07	1.17 ± 0.20	2.16 ± 0.26
7	7.5 – 200	111	0.47 ± 0.08	0.36 ± 0.07	0.83 ± 0.14	1.30 ± 0.16
8	5 – 200	157	0.50 ± 0.07	0.35 ± 0.06	0.85 ± 0.12	1.56 ± 0.13
9	.75 – 2.5	463	0.78 ± 0.07	0.45 ± 0.06	1.22 ± 0.11	1.73 ± 0.10

Table 1: Time constants [s] of the stretched exponential fit to the averaged pre-peak (t_r) and post-peak (t_d) profiles. Peak flux [ph cm⁻² s⁻¹] is taken from BATSE database. N is the number of bursts in the given brightness interval.

Fits of all time profiles have a good χ^2 except that for the weakest sample (# 6). Its profile is apparently deformed. This deformation is partially associated with the low trigger efficiency of this sample and with effects of Poisson noise. Nevertheless these biases are insufficient to explain this deformation and a real deformation effect could be present in the shape of the weakest sample. An analysis of this effect is beyond the scope of this poster paper.

The strongest effect in the remaining samples is the time dilation of the decaying (post-peak) slope of the time profile. Comparing t_d for samples 1 and 9 we find the time dilation to be a factor $1.86^{+0.82}_{-0.57}$, where the 90% confidence interval is given. Comparing samples 7 and 9 gives a factor $1.66^{+0.68}_{-0.42}$. Varying the lower flux limit of the brightest sample from $F_p = 5$ ph cm⁻² s⁻¹ and upwards does not significantly change the magnitude of the time dilation effect. A careful estimate of the significance level of the time dilation using model simulations gives 0.985.

The rising (pre-peak) slope is, however, surprisingly stable. The variations of t_r do not exceed statistical errors. This leads to an increasing asymmetry ratio, t_d/t_r , for the weaker samples. The effect is significant comparing samples 1 and 9: $(t_d/t_r)_{\text{dim}}/(t_d/t_r)_{\text{bright}} = 1.48^{+0.55}_{-0.32}$ (90% confidence interval). The probability of sampling such ratios if the asymmetry was constant is $4 \cdot 10^{-3}$.

The time dilation of $t_r + t_d$ has a smaller, but still acceptable significance when comparing samples 7 and 9. The “dim/bright” ratio becomes $1.47^{+0.63}_{-0.36}$. The probability for zero time dilation is 0.01.

4. INTERPRETATION OF CORRELATIONS USING THE PULSE AVALANCHE MODEL

The pulse avalanche model is based on the assumption that the well-shaped stretched exponential time profile results from a simple stochastic process responsible for the generation of time histories of GRBs. Then the diversity of GRB’s time histories arise as different random realizations of the same stochastic process at approximately the same parameters. The important requirement is a near-criticality

of the process - then it provides a large variety of individual bursts behaviours.

This idea was implemented as a near-critical chain reaction of events (of still unknown nature, it could, e.g., be reconnections of turbulent magnetic field), where each event is associated with one pulse of gamma-ray emission. Then, in a near critical regime, one spontaneous pulse can give rise to a long cascade of secondary pulses piling up into a complex chaotic event, or, depending on chance, no further pulses may result and we will instead see a simple single pulse event.

With a proper scaling of time delays between pulses and a proper spectrum of spontaneous pulses (flicker noise), the model successfully reproduces the stretched exponential profile (see Figure 3) as well as the autocorrelation function. There is also qualitative agreement with the duration distribution, the ratio of the number of simple and complex bursts is reproduced, and the model even produces the visual impression of real bursts. For more details see Stern & Svensson (1996).

Just two simple assumptions of those implemented in the pulse avalanche model are needed to demonstrate that all correlations described above are very natural. GRBs consist of a number of pulses of different durations but similar shapes. Let all these pulses have locally independent sources of energy. Then if two pulses coincide in time, their amplitudes sum up. In a complex event, hundreds of pulses are piling up, increasing the peak brightness by up to an order of magnitude. Then, if a pulse is a kind of standard candle, simple events are intrinsically weak and complex events are intrinsically bright.

At the same time, simple events are asymmetric just because a single pulse is asymmetric (e.g., Norris et al. 1996) with a sharp rise and a slower decay. This asymmetry is washed out in complex events where the position of the highest peak is more or less random among many overlapping pulses.

To demonstrate this we simulated a large sample of “bursts” using model parameters which gave an approximate agreement with the stretched exponential average time profile for the sample of all real bursts. The results are summarized in Table 2. We see that the asymmetry ratio, t_d/t_r , increases with decreasing peak flux.

Peak flux	t_d	t_r	$t_r + t_d$	t_d/t_r
0 - ∞	0.66	0.41	1.07	1.61
3 - ∞	0.75	0.68	1.43	1.10
0.8 - 3	0.72	0.50	1.22	1.44
0 - 0.8	0.50	0.19	0.69	2.63

Table 2: Time constants of the simulated bursts in different “intrinsic brightness” intervals. The amplitude of the single pulse is sampled uniformly from the interval $[0, 1]$.

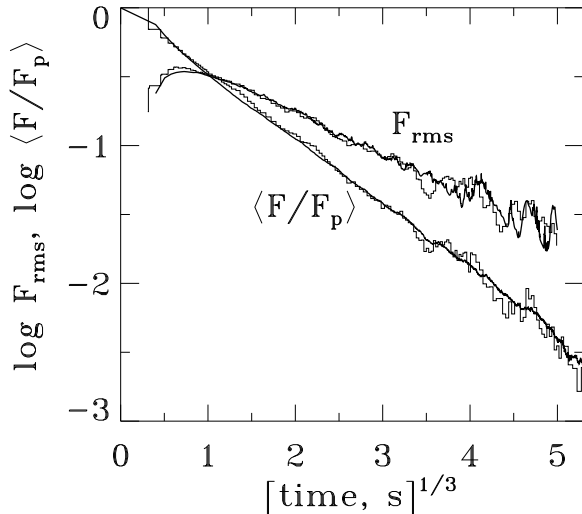


Figure 3: Comparison between observed and simulated average post-peak time profiles of GRBs. Thin-line histogram labelled $\langle F/F_p \rangle$ shows the average peak-aligned post-peak time profile for the 598 useful BATSE-3 events as the fractional flux, $\langle F/F_p \rangle$ vs. $t^{1/3}$, where F_p is the peak flux and $t = 0 - 150$ s is the time since the strongest peak. Thick curve labelled $\langle F/F_p \rangle$ is the average peak-aligned time profile for 5000 simulated time profiles. The set of curves labelled F_{rms} are the rms deviations of individual peak-aligned time profiles, $F_{\text{rms}} \equiv [\langle (F/F_p)^2 \rangle - \langle F/F_p \rangle^2]^{1/2}$, for both real (thin line histogram, 598 events) and simulated (thick curve, 5000 events) time profiles. Further details are given by Stern (1996) and Stern & Svensson (1996).

5. CONCLUSIONS

Besides the time dilation effect, observed in many previous works (e.g., Norris et al. 1994) we also see a dependence of the profile asymmetry on brightness and this effect is of the same order of magnitude as the time dilation itself.

A correlation of such a kind cannot be due to spectral redshifts. We find that strong events have slightly smaller asymmetry in the higher energy bands, (LAD channels 4 and 3) than in the lower energy bands (LAD channels 1 and 2). Redshifting the softer part of the spectrum below the detector threshold would then give rise to more symmetric, rather than asymmetric profiles. Details will be published elsewhere.

The effect of trigger efficiency is negligible for the brightness groups considered here. Also one can

hardly find an evolutionary factor that would change the asymmetry. One can suggest that there exist two separate classes of GRBs with different degree of asymmetry, which are differently distributed in space (separate classes of *long* bursts are required as short bursts do not contribute to the asymmetry). But such a suggestion seems too arbitrary, too radical, and unnecessary as there exists a much simpler explanation.

The simplest explanation is that the observed correlation is a consequence of an intrinsic correlation between shape and brightness as described above. The necessary condition for such a correlation to be observable is a significant deviation from a power law for the GRB distribution over luminosity distance. This would allow intrinsically strong events to dominate in the brightest observational range. The observed $\log N - \log P$ distribution is actually curved (Meegan et al. 1996) and this is natural if the distance distribution covers both Euclidean and $z \sim 1$ regions which have different luminosity distance scalings.

Maybe our detection of a strong shape - brightness correlation imposes a stronger constraint on the curvature of the true radial distribution of GRBs than what follows from the observed $\log N - \log P$ distribution. Detailed studies are, however, required to formulate this intuitive conclusion at a quantitative level.

As one kind of correlation has been observed, other kinds of intrinsic correlations may also be observable and this causes a problem for the cosmological interpretation of the time dilation effect. This problem, considered by Brainerd (1994), arises from unavoidable correlations between peak luminosity and time scales caused by different bulk Lorentz factor in the sources of different bursts. This effect can mimic both cosmological time dilation and spectral redshift.

However, if our interpretation using the pulse avalanche model is valid we must conclude that the real time dilation is larger than that obtained from Table 1. Actually, within the pulse avalanche framework, intrinsically weak events are not only more asymmetric, but they are also narrower (see column $t_r + t_d$ in Table 2). This is a new correction that increases the real time dilation more than the correction arising from spectral redshift (see Norris et al. 1994). The corrected time dilation could exceed a factor 2 and it could be caused by different effects, including the cosmological one. Unfortunately, the task of extracting the cosmological component from the total time dilation seems extremely difficult.

ACKNOWLEDGMENTS

We acknowledge support from the Swedish Royal Academy of Sciences, the Swedish Natural Science Research Council (in particular a postdoctoral fellowship for J.P.), and a NORDITA Nordic Project grant. This research used data obtained from the HEASARC Online Service provided by NASA/GSFC.

REFERENCES

- Brainerd, J. J. 1994, ApJ, 428, L1
- Meegan, C. A., et al. 1996, ApJS, 106, 65
- Mitrofanov, I. G., Chernenko, A. M., Pozanenko, A. S., Paciesas, W. S., Kouveliotou, C., Meegan, C. A., Fishman, G. J., Sagdeev, R. Z. 1994, in G. J. Fishman, J. J. Brainerd, K. C. Hurley (eds), Proc. of the Second Huntsville workshop on Gamma Ray Bursts, AIP, New York, 187
- Mitrofanov, I. G., et al. 1995, Astronomy Reports, 39, 305
- Norris, J. P., Nemiroff, R. J., Scargle, J. D., Kouveliotou, C., Fishman, G. J., Meegan, C. A., Paciesas, W. S., Bonnell, J. T. 1994, ApJ, 424, 540
- Norris, J. P., Nemiroff, R. J., Bonnell, J. T., Scargle, J. D., Kouveliotou, C., Paciesas, W. S., Meegan, C. A., Fishman, G. J. 1996, ApJ, 459, 393
- Paczyński, B. 1992, Nature, 355, 521
- Piran, T. 1992, ApJ, 389, L45
- Stern, B. E. 1996, ApJ, 464, L111
- Stern, B. E., Svensson, R. 1996, ApJ, 469, L109
- Stern, B. E., Poutanen, J., Svensson, R. 1997, in preparation